



Syntheses and conformational analyses of new naphth[1,2-*e*][1,3]oxazino[3,2-*c*]quinazolin-13-ones

Renáta Csütörtöki^a, István Szatmári^a, Andreas Koch^b, Matthias Heydenreich^b, Erich Kleinpeter^{b,*}, Ferenc Fülöp^{a,*}

^a Institute of Pharmaceutical Chemistry and Stereochemistry Research Group of Hungarian Academy of Sciences, University of Szeged, H-6720 Szeged, Eötvös u. 6, Hungary

^b Department of Chemistry, University of Potsdam, Karl-Liebknecht-Str. 24-25, D-14476 Potsdam (Golm), Germany

ARTICLE INFO

Article history:

Received 28 February 2012

Received in revised form 5 April 2012

Accepted 6 April 2012

Available online 14 April 2012

Keywords:

Naphthoxazinoquinazolinones

Aminonaphthols

NMR spectroscopy

Conformational analysis

Theoretical calculations

Ring current effect

ABSTRACT

The syntheses of naphth[1,2-*e*][1,3]oxazino[3,2-*c*]quinazolin-13-one derivatives (**3a–f**) were achieved by the solvent-free heating of benzyloxycarbonyl-protected intermediates (**2a–f**) with MeONa. For intermediates **2a–f**, prepared by the reactions of substituted aminonaphthols with benzyl *N*-(2-formylphenyl)carbamate, not only the expected *trans* ring form **B** and chain form **A**¹, but also the re-arranged chain form **A**² as a new tautomer were detected in DMSO at room temperature. The quantity of **A**² in the tautomeric mixture was changed with time.

Conformational analyses of the target heterocycles **3a–f** by NMR spectroscopy and accompanying theoretical calculations at the DFT level of theory revealed that the oxazine ring preferred a twisted chair conformation and the quinazolinone ring was planar. Besides the conformations, both the configurations at C-7a and C-15 and the preferred rotamers of the 1-naphthyl substituent at C-15 were assigned, which allowed evaluation of the aryl substituent-dependent steric hindrance in this part of the molecules. Configurational assignments were corroborated by quantifying the ring current effect of 15-aryl in terms of spatial NICS.

© 2012 Elsevier Ltd. All rights reserved.

1. Introduction

The Mannich reaction¹ is an important C–C bond formation reaction, that is, widely used in the syntheses of secondary and tertiary amine derivatives and as a key step in the syntheses of many bioactive molecules and complex natural products.² This reaction basically involves the addition of a carbon nucleophile to an iminium ion, resulting in a secondary or tertiary amine derivative, depending on the nature of the substrate used. One of its special variations is the modified Mannich reaction, in which electron-rich aromatic compounds, such as 1- or 2-naphthol are applied.³ In consequence of the two or more functional groups in the structure of the Mannich bases prepared via such modified reactions, one of the most important areas of application of these aminonaphthol derivatives is the synthesis of new heterocycles.³ Naphth[1,2-*e*][1,3]oxazino[3,4-*c*][1,3]benzoxazine and naphth[1,2-*e*][1,3]oxazino[3,2-*c*][1,3] benzoxazine derivatives have been prepared by the insertion of an additional hydroxy group through the reactions of aminonaphthols with salicylaldehyde,⁴

or by starting the synthesis from salicylaldehyde, leading to 1-(amino(2-hydroxyphenyl)methyl)-2-naphthol, followed by ring closure with oxo compounds.⁵ The syntheses of 8-substituted 10,11-dihydro-8*H*,15*bH*-naphth[1,2-*e*][1,3]oxazino[4,3-*a*]isoquinolines have been achieved through the cyclization of 1-(β-hydroxynaphthyl)-1,2,3,4-tetrahydroisoquinoline with formaldehyde, phosgene, *p*-nitrobenzaldehyde or *p*-chlorophenyl isothiocyanate,⁶ and the syntheses of naphth[1,2-*e*][1,3]oxazino[2,3-*a*]isoquinolines via unexpected reactions between 1-aminobenzyl-2-naphthol analogues and 6,7-dimethoxy-3,4-dihydroisoquinoline were recently described.⁷

We earlier reported the syntheses and conformational analyses of naphth[1,2-*e*][1,3]oxazino[3,4-*c*]quinazolinone derivatives from 1-(amino(2-aminophenyl)methyl)-2-naphthol, which was prepared by the reactions of 2-naphthol, 2-nitrobenzaldehyde and *tert*-butyl carbamate or benzyl carbamate.⁸ In order to investigate the influence of the anellation on the conformation of naphth[1,2-*e*][1,3]oxazinoquinazolines, our present aims were to synthesize new naphth[1,2-*e*][1,3]oxazino[3,2-*c*]quinazolinone derivatives, and to achieve the conformational analyses of these new polycyclic compounds by NMR spectroscopy and accompanying molecular modelling.

Quinazolinone derivatives have attracted considerable attention in view of the broad range of their pharmacological

* Corresponding authors. Tel.: +49 331 977 5210/5211; fax: +49 331 977 5064; e-mail addresses: ekleinp@uni-potsdam.de (E. Kleinpeter), fulop@pharm.u-szeged.hu (F. Fülöp).

activities, e.g., analgesic, anti-inflammatory, antibacterial, anti-cancer, sedative, vasodilator, anticonvulsant and antihypertensive activities.⁹

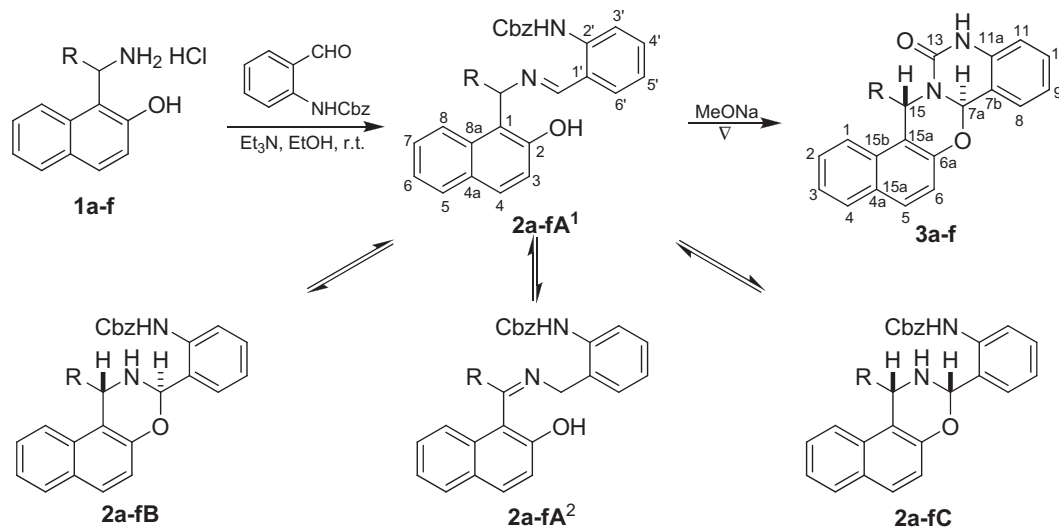
2. Results and discussion

2.1. Syntheses

For the synthesis of the proposed naphthoxazinoquinazolines, the preparations of 2-(2,3-dihydro-1*H*-naphth[1,2-*e*][1,3]oxa-

benzyloxycarbonyl-protected intermediates (**2a** and **2c**, Scheme 1). The mixtures were stirred for 2–4 days at room temperature, during which white crystals separated out. The crystalline products (**2a** and **2c**) were filtered off and washed with cold EtOH.

Our efforts to remove the protecting group either by catalytic (Pd/C) hydrogenation at atmospheric pressure or with 33% HBr/AcOH at room temperature led to the decomposition of **2a** and **2c** instead of formation of the desired amino derivatives. In additional experiments, the benzyloxycarbonyl-protected intermediates (**2a** and **2c**) were heated with MeONa (30 mol %) under solvent-free



R = H: **a**; *p*-Cl-Ph: **b**; Ph: **c**; *p*-OMe-Ph: **d**; 1-Nph: **e**; 2-Nph: **f**

Scheme 1. Syntheses of naphthoxazinoquinazolin-13-ones (**3a–f**).

zin-3-yl)aniline and 2-(1-phenyl-2,3-dihydro-1*H*-naphth [1,2-*e*][1,3]oxazin-3-yl)aniline as starting materials were planned. In our initial experiments, we attempted to prepare the target compounds through the condensations of 1-aminomethyl-2-naphthol or 1-aminobenzyl-2-naphthol with 1.1 equiv of 2-aminobenzaldehyde. However, because of the low reactivity of 2-aminobenzaldehyde (which can be explained by the presence of its imino mesomer structure¹⁰), there was no conversion. An attempt was made to shift the equilibrium towards the aldehyde function by using 1.5 equiv of Et₃N or HCl/EtOH, but even on the use of different reaction conditions (in EtOH at room temperature, or the application of microwave irradiation in EtOH at 60–90 °C), the target compounds could not be isolated, e.g., at room temperature there was no conversion, while the higher temperatures led to decomposition of the starting aminonaphthol.

In further experiments, the condensations of 1-aminomethyl-2-naphthol or 1-aminobenzyl-2-naphthol with 1.1 equiv of 2-nitrobenzaldehyde were attempted in MeOH in order to synthesize 2-(2,3-dihydro-1*H*-naphth[1,2-*e*][1,3]oxazin-3-yl)aniline and 2-(1-phenyl-2,3-dihydro-1*H*-naphth[1,2-*e*][1,3]oxazin-3-yl)aniline. These reactions did lead to the formation of the expected nitro derivatives. However, although the transformation of the nitro function to an amino group should have been achieved for the syntheses of 2-aminophenyl-substituted naphthoxazines, neither catalytic (Pd/C) hydrogenation nor reduction with Fe powder in the presence of concentrated HCl resulted in isolation of the desired amino derivatives, and after even a short reaction time decomposition of the starting naphthoxazines was observed on TLC.

As a new synthetic strategy, aminonaphthols were reacted with benzyl *N*-(2-formylphenyl)carbamate to afford the corresponding

conditions at their melting temperatures. After reaction times of 10 and 30 min, when TLC showed no presence of the starting materials, the reaction mixtures were cooled down and the products (**3a** and **3c**) were isolated by treatment with EtOH. This synthetic pathway was extended for the preparation of naphthoxazinoquinazolinones containing different aryl substituents at position 15 (*p*-Cl-Ph: **3b**, *p*-OMe-Ph: **3d**, 1-naphthyl: **3e**, and 2-naphthyl: **3f**) (Scheme 1). It should be mentioned that in the cases of **3d** and **3f** a doubled amount of MeONa (60 mol %) increased the yields (from 31% to 60% for **3d**, and from 37% to 51% for **3f**; Table 5). For **3f**, a different work-up procedure was applied; the solid residue was extracted with EtOAc and dried (Na₂SO₄), and after evaporation of the solvent the residue was crystallized from a mixture of *n*-hexane:EtOAc.

In CDCl₃ at 300 K, **2a–f** can participate in three-component tautomeric mixtures containing diastereomeric ring forms (**B** and **C**) besides the chain form (**A**).¹¹ Because of the low solubility of intermediates **2a–f** in CDCl₃, the NMR spectra were recorded in DMSO. The total assignment of **2c** revealed the presence of a new tautomeric chain form (**A**²) besides the *trans* ring form **B** and chain form **A**¹. Through the use of 2D NMR techniques, the structure of **A**² was identified as a tautomeric form of **A**¹, in which the imine double bond is in an α position relative to the naphthyl ring, as depicted in Scheme 1. To establish whether this unexpected rearrangement is influenced by the nature of substituent R, the NMR spectra of **2a,b** and **2d–f** (Table 1, entries 1, 4, 14, 19 and 24) were recorded on solutions of 15 mg of crystals in 700 μ L of deuterated DMSO. The ratio of **A**¹ to **A**² did differ, but our attention then focused on the influence of time. Thus, the spectra of **2b–f** were recorded after the solutions had been allowed to stand for 4 h or 3, 4 or 7 days. In the

Table 1
Tautomeric ratios for **2a–f** in DMSO at 300 K

Entries	R	Time ^a	A ¹ (%)	A ² (%)	B (%)
1	H 2a	0	100	—	—
2		7 days	82.2	—	17.8
3		12 days	76.9	—	23.1
4	<i>p</i> -Cl-Ph 2b	0	91.7	—	8.3
5		4 h	81.1	11.1	7.8
6		3 days	40.5	54.1	5.4
7		4 days	30.4	67.2	2.4
8		7 days	18.6	80.1	1.3
9	Ph 2c	0	82.6	10.5	6.9
10		4 h	65.3	28.8	5.9
11		3 days	38.3	57.7	4.0
12		4 days	34.2	63.2	2.6
13		7 days	27.6	70.2	2.2
14	<i>p</i> -OMe-Ph 2d	0	89.4	—	10.6
15		4 h	76.7	14.0	9.3
16		3 days	12.4	86.3	1.3
17		4 days	5.9	93.1	1.0
18		7 days	2.8	97.2	—
19	1-Nph 2e	0	66.7	—	33.3
20		4 h	67.4	—	32.6
21		3 days	66.4	—	33.6
22		4 days	67.4	—	32.6
23		7 days	67.0	—	33.0
24	2-Nph 2f	0	90.9	0.5	8.6
25		4 h	53.9	38.9	7.2
26		3 days	19.4	76.2	4.4
27		4 days	16.3	83.7	—
28		7 days	14.8	85.2	—

^a The duration of standing after dissolution of the samples.

case of **2a**, form **A²** could not be detected even after 12 days (Table 1, entries 1–3). The reason for this is that, in the lack of an aromatic ring system, there is no possibility of conjugation with the C=N double bond in **A²**. Further proof of the presence of conjugation in form **A²** is that, in the case of **2e**, containing a 1-naphthyl ring, the rearranged form **A²**, could not be detected even after 7 days. This can be explained by the hindered rotation of the naphthyl ring, which restricts conjugation of the aromatic system with the C=N double bond.

Table 1 shows that the standing time has a characteristic influence on the tautomeric ratios. In all cases (**2b–d,f**), the amount of **A²** increases, while those of **B** and **A¹** decrease as time passes. It can also be concluded from Table 1 that the formation of **A²** (after standing for 7 days) is the highest for the electron-donating substituent *p*-OMe. To prove the reversibility of the process in DMSO (the presence of a tautomeric equilibrium), 40 mg of **2c** was dissolved in DMSO (2 mL, corresponding to the concentration used for the NMR measurements) and the solution was left to stand at room temperature for 7 days. A sample from this mixture was then evaporated to dryness, and dissolved again in deuterated DMSO, after which its NMR spectrum was run. The tautomeric composition observed was similar to that after the dissolution of crystalline **2c**.

Even if **2a–fC** could not be isolated the minimum-energy structure of this compound and of the corresponding isomers **2a–fB** were computed and the results for **2bB** and **2bC**, respectively, are given in Fig. 1a. *Trans*-isomers (**2a–fB**) were found to be between 1.28 kcal/mol and 3.43 kcal/mol more stable in agreement with the experiment. The *trans* position of the protons H-7a and H-15 is readily visible (cf. Fig. 1a); the corresponding NOE cannot be developed as aforementioned (*vide supra*).

During the ring closure reaction of **2b–f** with MeONa, the formation of two diastereomers is possible; the diastereomeric ratio was therefore checked by NMR spectroscopy on the crude products. It was found that only one diastereomer was present in all five cases. The preliminary NOE check on purified **3b–f** adequately proved the *trans* arrangement of H-15 and H-7a (Scheme 1). The formation of only one diastereomer (*trans*) in case of naphthoxazinoquinazolinones **3b–f** can be explained by the aid of the steric hindrance of bulky aryl substituents at position 15.

2.2. Conformational analysis

The conformational search protocol involved PM3 geometry minimization, followed by geometry optimization without restrictions. All calculations were carried out by using the Gaussian 09 program package.¹² Density functional theory calculations were

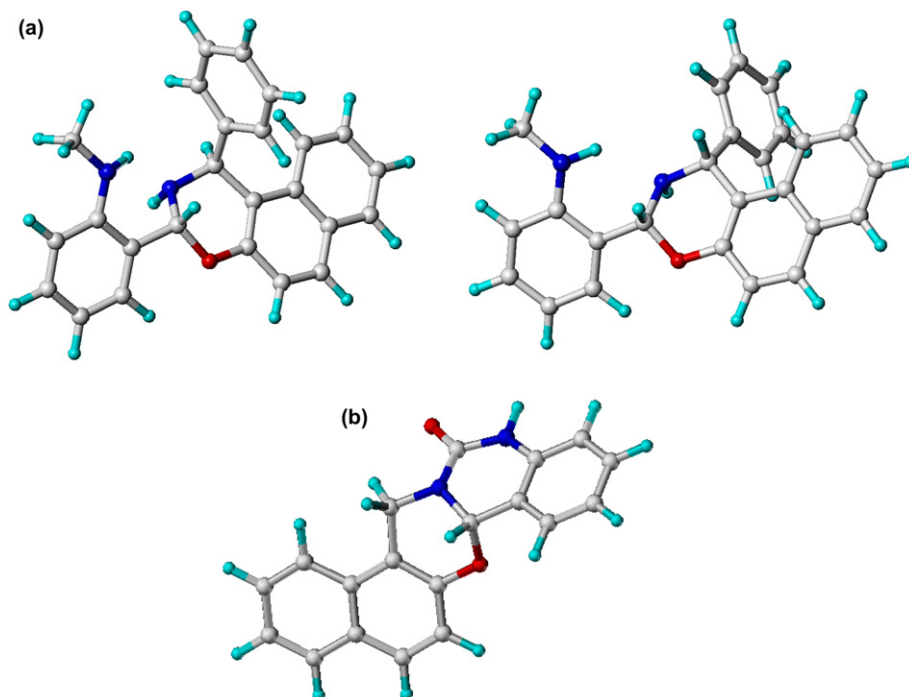


Fig. 1. a. Minimum-energy structure of **2bB** and **2bC**(NHMe instead of NHCOOCH₂Ph); b. Global minimum-energy structure of **3a**.

performed at the B3LYP/6-31C** level of theory.^{13,14} The molecular modelling software package SYBYL 7.3 was used to display results and geometries.¹⁵ As the NMR measurements were recorded in DMSO, the energies of the participating conformers were calculated with consideration of the effect of the solvent via the dielectric constant $\epsilon=46.7$. All configurations of **3a–f** were studied at the DFT level of theory with respect to the preferred conformers or conformational equilibria. In **7aH,12H,15bH**-naphth[1,2-*e*][1,3]oxazino[3,2-*c*]quinazolin-13-one (**3a**), only one chiral centre is present. Fig. 1b shows the global minimum-energy structure of **3a**.

In consequence of the presence of the aryl substituents at position 15, the remaining compounds **3b–f** contain two chiral centres. Theoretical calculations were performed for all of the stereoisomers as regards both the configurations of C-15 and C-7a and the ring interconversions of the two non-aromatic ring moieties. To begin with compounds **3b–d**, the results of the optimization are given in Table 2. It can be concluded from the relative energy values that the *trans* arrangement of H-15 and H-7a is favourable for **3b–d** (Table 2). The lack of NOESY interaction between H-15 and H-7a indirectly proved the *trans* arrangement, which is indicated by the theoretical calculations at the DFT level.

Table 2
Calculated energy differences for **3b–d**

	Optimized geometry	C-15	C-7a	ΔE^a (kcal/mol)	ΔE^b (kcal/mol)
3b	<i>trans</i>	<i>S</i> [*]	<i>R</i> [*]	0	0
	<i>cis</i>	<i>S</i> [*]	<i>S</i> [*]	5.27	5.10
3c	<i>trans</i>	<i>S</i> [*]	<i>R</i> [*]	0	0
	<i>cis</i>	<i>S</i> [*]	<i>S</i> [*]	5.56	5.32
3d	<i>trans</i>	<i>S</i> [*]	<i>R</i> [*]	0	0
	<i>cis</i>	<i>S</i> [*]	<i>S</i> [*]	5.79	5.57

^a In the gas phase.

^b In DMSO as solvent.

Fig. 2 depicts the minimum-energy structures of the *trans* and *cis* diastereomers of **3b–d**.

As a result of the restricted rotation of the naphthyl substituents at position 15 around the C-15–C-1' bond in **3e**, and around the C-15–C-2' bond in **3f**, four conformers were obtained after the geometry optimization, i.e., structures with *syn* and *anti* positions of H-15 and C-2' in **3e** and of H-15 and C-1' in **3f** (cf. Table 3).

The theoretical results in Table 3 demonstrate that the *trans* arrangement of H-15 and H-7a is favourable for both **3e** and **3f**. This is the case in both the *trans* and the *cis* diastereomers of **3e** (*anti* position of H-15 and C-2'). In the *trans*_I and *cis*_{II} geometries of **3e** N-14 is not planar and its relative configuration is *R*^{*}, while in both the *trans*_{II} and the *cis*_I geometries of **3e**, N-14 was found to be planar as in the cases of **3a–d** and **3f**. The sterically hindered rotation of the 1-naphthyl substituent around the C-15–C-1' bond led to the energy difference between the *trans*_I and *trans*_{II} forms of **3e** being relatively high: 4.92 kcal/mol (cf. Table 3). Fig. 3 illustrates the minimum-energy structures of the *trans* and *cis* diastereomers of **3e**.

In the *trans* diastereomers of **3f**, the *anti* position of H-15 and C-1' was found to be preferred, in contrast with the *syn* position in the *cis* diastereomers. The energy difference between the *trans*_I and *trans*_{II} forms of **3f** was relatively low: 0.78 kcal/mol (Table 3); as expected, the rotation of the 2-naphthyl substituent around the C-15–C-2' bond is less sterically hindered than that of the 1-naphthyl substituent around the corresponding C-15–C-1' bond. Fig. 4 depicts the minimum-energy structures of the *trans* and the *cis* diastereomers of **3f**.

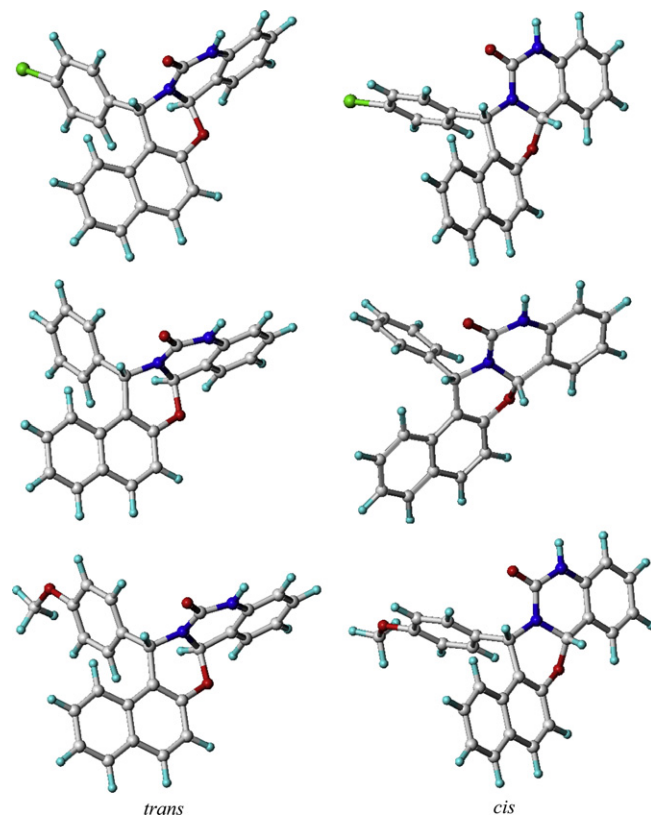


Fig. 2. Minimum-energy structures of the *trans* and *cis* diastereomers of **3b–d**.

Table 3
Calculated energy differences for **3e** and **3f**

	H-15–C-2'/ H-15–C-1'	Optimized geometry	C-15	C-7a	ΔE^a (kcal/mol)	ΔE^b (kcal/mol)
3e	<i>anti</i> ^c	<i>trans</i> _I	<i>S</i> [*]	<i>R</i> [*]	0	0
	<i>syn</i>	<i>trans</i> _{II}	<i>S</i> [*]	<i>R</i> [*]	4.88	4.92
	<i>anti</i>	<i>cis</i> _I	<i>S</i> [*]	<i>S</i> [*]	8.27	8.09
	<i>syn</i> ^c	<i>cis</i> _{II}	<i>S</i> [*]	<i>S</i> [*]	9.21	8.78
3f	<i>anti</i>	<i>trans</i> _I	<i>S</i> [*]	<i>R</i> [*]	0	0
	<i>syn</i>	<i>trans</i> _{II}	<i>S</i> [*]	<i>R</i> [*]	0.79	0.78
	<i>syn</i>	<i>cis</i> _I	<i>S</i> [*]	<i>S</i> [*]	5.66	5.40
	<i>anti</i>	<i>cis</i> _{II}	<i>S</i> [*]	<i>S</i> [*]	6.25	5.98

^a In the gas phase.

^b In DMSO as solvent.

^c In these structures, N-14 was found to be not planar and its relative configuration was *R*^{*}.

In order to illustrate the differences in the sterically hindered rotation of the aryl substituents (phenyl, 1-naphthyl or 2-naphthyl) around the C-15–C-1' or the C-15–C-2' bond in **3c,e** and **3f**, the energy was calculated with respect to the deviations of the torsion angle (in 5° steps up to -30° or +30°, respectively) from the corresponding values in the minimum-energy structures. The energy values obtained are plotted versus the torsion angle in **3c,e** and **3f** in Fig. 5. It is readily concluded that, for a given torsion angle deviation, the 1-naphthyl substituent requires a higher energy than the 2-naphthyl or phenyl substituents. In turn, 2-naphthyl requires less energy than 1-naphthyl, while the symmetrical phenyl ring suffers the lowest steric hindrance.

2.3. Anisotropic effects

In order to demonstrate the stereochemistry of the naphth[1,2-*e*][1,3]oxazino[3,2-*c*]quinazolinone derivatives (obtained by

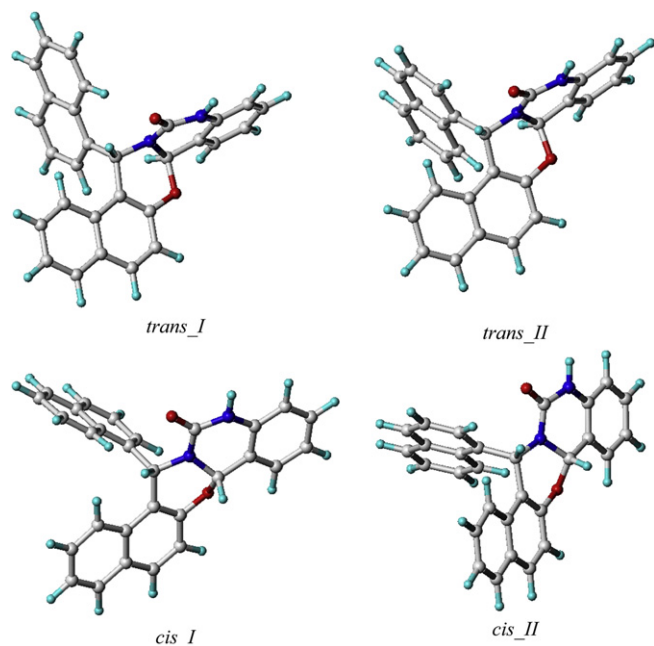


Fig. 3. Minimum-energy structures of the *trans* and *cis* diastereomers of **3e**.

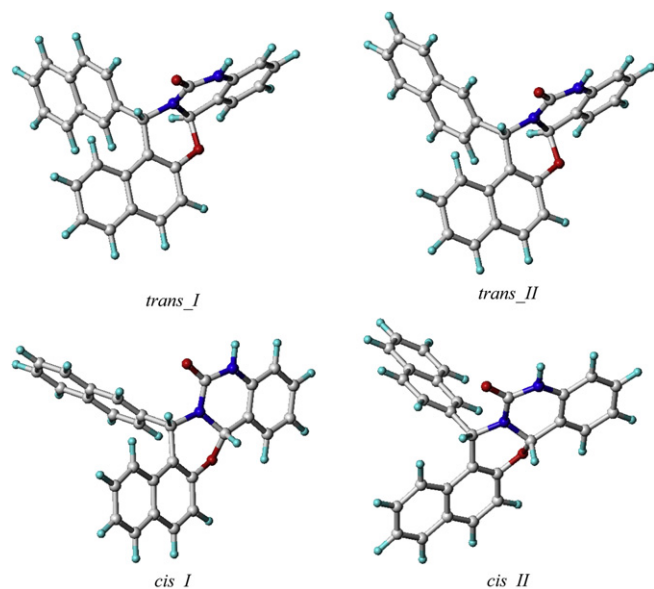


Fig. 4. Minimum-energy structures of the *trans* and *cis* diastereomers of **3f**.

means of DFT calculations and proved only indirectly through the lack of NOE (H-7a...H-15) information), the ring current effects of the 15-aryl substituents on H-1 in **3c,e** and **3f** were computed. For this purpose, the spatial NICS approach¹⁶ was employed. The through-space NMR shieldings (TSNMRSSs) can be visualized¹⁶ as iso-chemical-shielding surfaces (ICSSs) and employed to quantify the anisotropic effects of functional groups on proton chemical shifts (to determine the stereochemistry of nuclei proximal to the functional group),^{5,17–27} in order to separate the anisotropic effects of functional groups from the influence of steric hindrance on the same proton chemical shifts,²⁸ and to visualize and quantify planar^{29,30} or spherical (anti)aromaticity^{31–33} and chelatoaromaticity.³⁴

From the optimized geometries of **3c,e** and **3f**, the TSNMRSSs of the aryl moieties on C-15 were calculated, visualized by ICSSs of

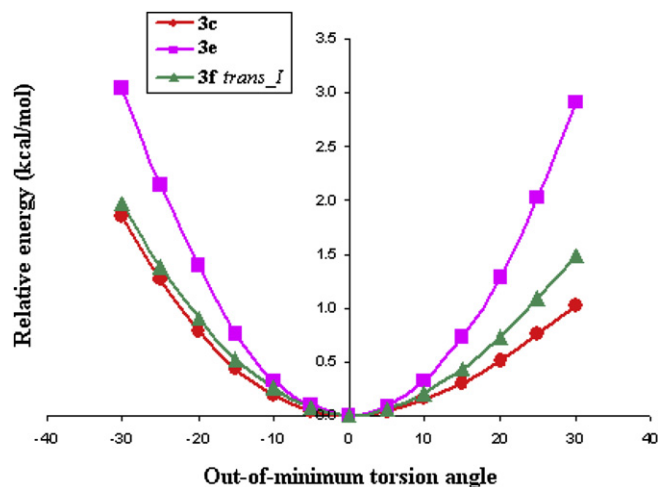


Fig. 5. Plots of ΔE for **3c,e** and **3f** versus the torsion angle of the rotation about C-15–C-1' or C-15–C-2'.

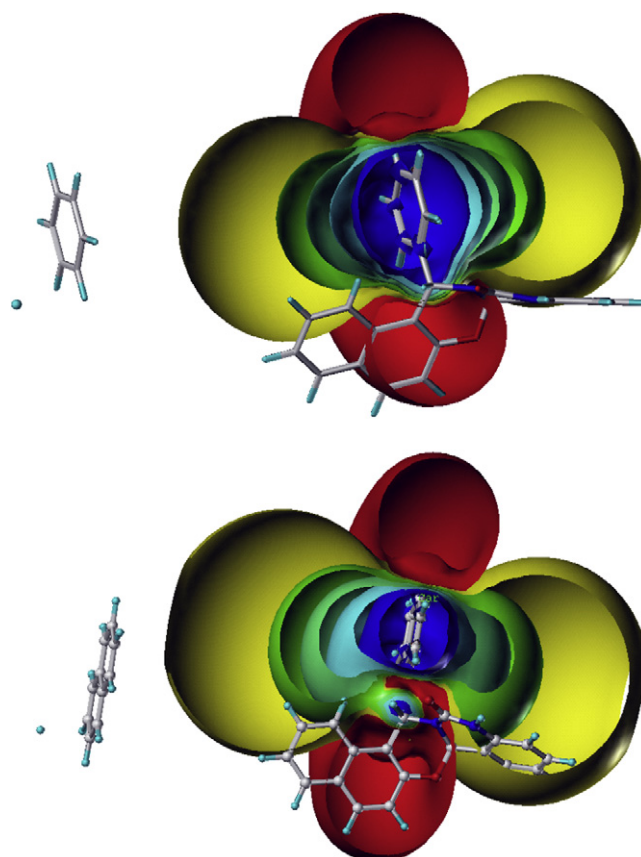


Fig. 6. Ring current effects of the phenyl ring in **3c** and the 1-naphthyl ring in **3e** on H-1.

various sizes and directions (cf. Fig. 6 for **3c** (phenyl) and **3e** (naphthyl ring system), respectively) and finally the corresponding anisotropic effect of the 15-aryl moiety on H-1 was computed quantitatively. The corresponding values (as shielding values, negative for deshielding and positive for the shielding of H-1) are given in Table 4, together with the H-1 chemical shift in **3a** as reference.

The coincidence is very good: the anisotropic effect of the 15-aryl moiety proves to be ~ 0.5 ppm, in complete agreement with the experiment, and proves the stereochemistry of the naphth[1,2-*e*][1,3]oxazino[3,2-*c*]quinazolinone derivatives **3c,e** and **3f**.

Table 4

Experimental differences in the chemical shifts δ /ppm of H-1 and the anisotropic effects of 15-aryl in **3c,e,f** σ /ppm

Comp.	δ_{exp} (H-1)	$\Delta\delta_{\text{exp}}$ /ppm	σ_{calcd} /ppm
3a	7.84	0	—
3c	7.39	0.45	0.56
3e	7.22	0.62	0.55
3f	7.45	0.39	0.49

3. Conclusions

The benzyloxycarbonyl-protected intermediates (**2a–f**) were synthesized by the reactions of substituted aminonaphthol derivatives (**1a–f**) with benzyl *N*-(2-formylphenyl)carbamate. When the NMR spectra of **2a–f** were recorded in DMSO, the spectra of **2b–d,f** revealed the presence of a new tautomeric chain form (**A²**) besides the *trans* ring form **B** and the chain form **A¹**. The ratio of **A¹–A²** was studied and found to depend on the time of standing. Compounds **2a–f** were transformed to naphth[1,2-*e*][1,3]oxazino[3,2-*c*]quinazolin-13-one derivatives (**3a–f**) by solvent-free heating with MeONa. The lack of a cross-peak between H-15 and H-7a in the NOESY NMR spectra of **3b–f** indirectly proved their *trans* arrangement, which was indicated by the DFT geometry optimization. Both the configurations and conformations of the naphth[1,2-*e*][1,3]oxazino[3,2-*c*]quinazolin-13-one derivatives **3b–f** were elucidated by theoretical calculations at the DFT level; the (C-15, C-7a) *trans*-isomers (in the cases of **3e,f**, *trans*_1) are preferred. The steric hindrance of the aryl substituents on C-15 was also studied and found to decrease in the sequence 1-naphthyl>2-naphthyl>phenyl. Finally, the anisotropic effect of the 15-aryl ring current on H-1 was calculated: the excellent agreement of the computational results and experiment proved the stereochemistry of the naphth[1,2-*e*][1,3]oxazino[3,2-*c*]quinazolin-13-one derivatives **3b–f** deduced from the theoretical calculations.

4. Experimental section

4.1. General

Melting points were determined on a Hinotek X-4 type melting point apparatus and are uncorrected.

The different conformations and configurations of the studied compounds were preoptimized with the PM3 Hamiltonian.³⁵ The B3LYP density functional method was selected for all calculations. The method was based on Becke's three-parameter hybrid functionals³⁶ and the correlation functional of Lee et al.³⁷ All optimizations were carried out without any restriction at this B3LYP/6-31G** level of theory.^{13,14} The self-consistent reaction field method (SCRF) and the polarizable continuum model (PCM) using the integral equation formalism variant (IEF-PCM) were applied to take solvent effects (DMSO) into account.³⁸ Visualization was carried out with the modelling software SYBYL 7.3¹⁵ and the program GaussView 2.0.³⁹

The ¹H and ¹³C NMR spectra were recorded in DMSO solutions in 5 mm tubes, at room temperature, on a Bruker Avance III spectrometer at 600.13 (¹H) and 150.61 (¹³C) MHz, with the deuterium signal of the solvent as the lock and TMS as internal standard. All spectra (¹H, ¹³C, gs-H, H-COSY, gs-HMQC, gs-HMBC and NOESY) were acquired and processed with the standard BRUKER software.

The low-resolution EI mass spectra were obtained with a GC–MS TRACE DSQ II mass spectrometer (Thermo Fisher Scientific Dreieich, Germany) with an electron energy of 70 eV and a source temperature of 180 °C, using a direct insertion probe with a DEP filament for positive ionization mode. The HRMS EI spectra were recorded with a GC/MS instrument with a time-of-flight mass

analyser (Micromass/Waters, Manchester, UK) in positive ion mode. The elemental compositions of the ions were determined by accurate mass measurements with standard deviation <5 ppm. Perfluorokerosene was used as reference compound and the mass resolution was 5000.

Starting aminonaphthols were synthesized according to literature methods: **1a–d**,¹¹ **1e**⁴⁰ and **1f**.⁴⁰ 2-Aminobenzaldehyde and benzyl *N*-(2-formylphenyl)carbamate were prepared on the basis of syntheses described in the literature.^{41,42} It should be mentioned that benzyl *N*-(2-formylphenyl)carbamate was earlier reported as a colourless oil,⁴² but in our experiment it was isolated as white crystals (mp: 60–62 °C; lit.⁴³ mp: 64–65 °C).

4.2. General method for the syntheses of benzyloxycarbonyl-protected intermediates **2a–f**

Et₃N (3.3 mmol) and benzyl *N*-(2-formylphenyl)carbamate (3.3 mmol) were added to a solution of the appropriate aminonaphthol hydrochloride (3 mmol) in EtOH (15 mL). The mixture was stirred for 2–4 days at room temperature, during which white crystals separated out. The crystalline products (**2a–f**) were filtered off and washed with cold EtOH (2 × 5 mL). After dissolution of the samples, the chain form **A¹** was found to be the major tautomer; the full assignment of the NMR signals is therefore described only for **A¹**, while for the minor forms **A²** and **B** only the characteristic signals are listed.

4.2.1. Compound 2a. White crystals, yield: 1.00 g (81%), mp: 172–174 °C. HR-EIMS: *m/z* calcd for C₂₆H₂₂N₂O₃: 410.1625, found 410.1622.

4.2.2. Compound 2aA¹ (major tautomer). ¹H NMR (600 MHz, DMSO) δ =5.07 (s, 2H, COOCH₂), 5.21 (s, 2H, NphCH₂), 7.09 (t, 1H, 5'-H, *J*=7.5 Hz), 7.20–7.26 (m, 5H, 3-H, 7-H, 6-H, 2''-H, 6''-H), 7.33–7.37 (m, 3H, 3''-H, 5''-H, 4''-H), 7.40 (t, 1H, 4'-H, *J*=7.9 Hz), 7.53 (d, 1H, 6'-H, *J*=7.9 Hz), 7.75 (d, 1H, 4-H, *J*=9.0 Hz), 7.79 (d, 1H, 5-H, *J*=9.0 Hz), 8.07 (d, 1H, 8-H, *J*=9.0 Hz), 8.22 (d, 1H, 3'-H, *J*=8.4 Hz), 8.65 (s, 1H, N=CH), 9.89 (br s, 1H, OH), 12.36 (s, 1H, NH). ¹³C NMR (150 MHz, DMSO): δ =53.6 (NphCH₂), 65.8 (COOCH₂), 115.2 (C-1), 117.3 (C-3'), 118.2 (C-3), 120.4 (C-1'), 121.9 (C-5'), 122.6 (C-6), 123.0 (C-8), 126.6 (C-7), 127.8 (C-2'', C-6''), 128.0 (C-4''), 128.1 (C-4a), 128.2 (C-5), 128.5 (C-3'', C-5''), 129.1 (C-4), 131.4 (C-4'), 133.3 (C-8a), 133.6 (C-6'), 136.4 (C-1''), 139.4 (C-2'), 153.1 (COH), 153.2 (COOCH₂), 164.8 (N=CH).

4.2.3. Compound 2aB (minor tautomer, characteristic signals). ¹H NMR δ =4.50 (s, 2H, COOCH₂), 4.74–5.74 (m, 2H, NphCH₂), 6.64 (s, 1H, NHCHO), 10.23 (br s, 1H, OH). ¹³C NMR δ =40.6 (NphCH₂), 63.0 (COOCH₂), 82.7 (NHCHO).

4.2.4. Compound 2b. White crystals, yield: 1.02 g (65%), mp: 178–179 °C. HR-EIMS: *m/z* calcd for C₃₂H₂₅ClN₂O₃: 520.1548, found 520.1551.

4.2.5. Compound 2bA¹ (major tautomer). ¹H NMR (600 MHz, DMSO) δ =5.19–5.31 (m, 2H, COOCH₂), 6.77 (s, 1H, PhCH), 6.83 (t, 1H, H-7, *J*=7.6 Hz), 7.03–7.08 (m, 1H, 6-H), 7.10 (t, 1H, 5'-H, *J*=7.6 Hz), 7.13–7.18 (m, 2H, 3''-H, 5''-H), 7.20–7.29 (m, 2H, 4''-H, H-3), 7.34–7.38 (m, 2H, 3'''-H, 5'''-H), 7.39–7.43 (m, 2H, 2''-H, 6''-H), 7.46 (t, 1H, 4'-H, *J*=7.9 Hz), 7.54–7.59 (m, 3H, 2'''-H, 6'''-H, 6'-H), 7.71 (d, 1H, 5-H, *J*=8.2 Hz), 7.76 (d, 1H, 4-H, *J*=8.9 Hz), 7.81 (d, 1H, 8-H, *J*=8.6 Hz), 8.28 (d, 1H, 3'-H, *J*=8.4 Hz), 8.71 (s, 1H, N=CH), 10.25 (br s, 1H, OH), 12.63 (s, 1H, NH). ¹³C NMR (150 MHz, DMSO): δ =65.9 (COOCH₂), 66.2 (PhCH), 117.4 (C-3'), 118.0 (C-3), 119.2 (C-1), 120.4 (C-1'), 122.1 (C-5'), 122.4 (C-6), 125.2 (C-8), 125.8 (C-7), 127.8 (C-4''), 127.9 (C-2'', C-6''), 128.5 (C-5, C-3''', C-5'''), 128.6 (C-3'', C-5''), 128.9 (C-4a), 129.1 (C-2''', C-6'''), 129.8 (C-4), 130.9 (C-8a), 132.0 (C-4'),

134.0 (C-6'), 135.0 (C-C1), 136.5 (C-1''), 139.6 (C-2'), 142.3 (C-1'''), 153.0 (COH), 153.3 (COOCH₂), 166.2 (N=CH).

4.2.6. Compound **2bA**² (minor tautomer, characteristic signals). ¹H NMR δ=4.35–4.49 (m, 2H, C=NCH₂), 5.08 (s, 2H, COOCH₂), 9.44 (br s, 1H, OH), 10.11 (br s, 1H, HNCOOCH₂). ¹³C NMR δ=54.5 (C=NCH₂), 65.8 (COOCH₂).

4.2.7. Compound **2bB** (minor tautomer, characteristic signals). ¹H NMR δ=4.70–4.75 (m, 1H, CHNHCH), 5.01–5.12 (m, 2H, COOCH₂), 5.61 (d, 1H, HNCHO, J=13.2 Hz), 5.67 (s, 1H, NphCHNH), 8.95 (br s, 1H, HNCOOCH₂). ¹³C NMR δ=52.0 (NphCHNH), 66.0 (COOCH₂), 78.5 (HNCHO).

4.2.8. Compound **2c**. White crystals, yield: 1.08 g (74%), mp: 150–152 °C. HR-EIMS: *m/z* calcd for C₃₂H₂₆N₂O₃: 486.1938, found 486.1941.

4.2.9. Compound **2cA**¹ (major tautomer). ¹H NMR (600 MHz, DMSO) δ=5.20–5.31 (m, 2H, COOCH₂), 6.77–6.82 (m, 2H, PhCH, 7-H), 7.02–7.11 (m, 2H, 6-H, 5'-H), 7.22–7.26 (m, 2H, 3'''-H, 5'''-H), 7.27–7.43 (m, 8H, 2'''-H, 6'''-H, 3-H, 3''-H, 5''-H, 2''-H, 6''-H, 4''-H), 7.46 (t, 1H, 4'-H, J=7.9 Hz), 7.55–7.60 (m, 2H, 6'-H, 4'''-H), 7.70 (d, 1H, 5-H, J=8.1 Hz), 7.74 (d, 1H, 4-H, J=9.0 Hz), 7.91 (d, 1H, 8-H, J=8.9 Hz), 8.28 (d, 1H, 3'-H, J=8.4 Hz), 8.74 (s, 1H, N=CH), 10.21 (br s, 1H, OH), 12.65 (s, 1H, NH). ¹³C NMR (150 MHz, DMSO): δ=66.1 (COOCH₂), 67.2 (PhCH), 117.5 (C-3'), 118.0 (C-3), 119.7 (C-1), 120.5 (C-1'), 122.1 (C-5'), 122.3 (C-6), 125.5 (C-8), 125.7 (C-7), 127.1 (C-2''', C-6'''), 127.4 (C-4'''), 127.8 (C-2'', C-6''), 128.3 (C-5), 128.4 (C-3'', C-5''), 128.5 (C-3''', C-5'''), 128.9 (C-4a), 129.6 (C-4), 130.3 (C-4''), 131.5 (C-8a), 131.9 (C-4'), 134.0 (C-6'), 136.7 (C-1''), 139.6 (C-2'), 143.3 (C-1'''), 152.9 (COH), 153.3 (COOCH₂), 165.9 (N=CH).

4.2.10. Compound **2cA**² (minor tautomer, characteristic signals). ¹H NMR δ=4.36–4.50 (m, 2H, C=NCH₂), 5.11 (s, 2H, COOCH₂), 9.60 (br s, 1H, OH), 10.06 (br s, 1H, HNCOOCH₂). ¹³C NMR δ=54.7 (C=NCH₂), 65.8 (COOCH₂). **2cB** (Minor tautomer, characteristic signals): δ=4.67–4.73 (m, 1H, CHNHCH), 4.99–5.10 (m, 2H, COOCH₂), 5.62 (d, 1H, HNCHO, J=13.3 Hz), 5.67 (s, 1H, NphCHNH), 8.97 (br s, 1H, HNCOOCH₂). ¹³C NMR δ=52.7 (NphCHNH), 65.9 (COOCH₂), 78.6 (HNCHO).

4.2.11. Compound **2d**. White crystals, yield: 0.90 g (58%), mp: 152–154 °C. HR-EIMS: *m/z* calcd for C₃₃H₂₈N₂O₄: 516.2044, found 516.2049.

4.2.12. Compound **2dA**¹ (major tautomer). ¹H NMR (600 MHz, DMSO) δ=3.69 (s, 3H, OCH₃), 5.19–5.32 (m, 2H, COOCH₂), 6.73 (s, 1H, PhCH), 6.78 (d, 2H, 3'''-H, 5'''-H, J=8.6 Hz), 6.83 (t, 1H, 7-H, J=8.0 Hz), 7.05 (t, 1H, 6-H, J=7.5 Hz), 7.10 (t, 1H, 5'-H, J=7.5 Hz), 7.18 (d, 2H, 2'''-H, 6'''-H, J=8.5 Hz), 7.28 (d, 1H, 3-H, J=8.7 Hz), 7.33–7.37 (m, 3H, 3''-H, 5''-H, 4''-H), 7.38–7.42 (m, 2H, 2''-H, 6''-H), 7.45 (t, 1H, 4'-H, J=7.9 Hz), 7.57 (d, 1H, 6'-H, J=7.5 Hz), 7.70 (d, 1H, 5-H, J=8.1 Hz), 7.73 (d, 1H, 4-H, J=9.0 Hz), 7.93 (d, 1H, 8-H, J=8.5 Hz), 8.27 (d, 1H, 3'-H, J=8.5 Hz), 8.72 (s, 1H, N=CH), 10.17 (br s, 1H, OH), 12.64 (s, 1H, NH). ¹³C NMR (150 MHz, DMSO): δ=55.1 (OCH₃), 66.1 (COOCH₂), 66.8 (PhCH), 113.7 (C-3''', C-5'''), 117.5 (C-3'), 118.1 (C-3), 119.8 (C-1), 120.5 (C-1'), 122.1 (C-5'), 122.3 (C-6), 125.5 (C-7), 125.6 (C-8), 127.1 (C-2''', C-6'''), 127.8 (C-2'', C-6''), 128.1 (C-5), 128.3 (C-4''), 128.5 (C-3'', C-5''), 128.9 (C-4a), 129.5 (C-4), 131.7 (C-8a), 131.8 (C-4'), 133.9 (C-6'), 135.1 (C-1'''), 136.5 (C-1''), 139.6 (C-2'), 152.8 (COH), 153.3 (COOCH₂), 157.7 (COCH₃), 165.6 (N=CH).

4.2.13. Compound **2dA**² (minor tautomer, characteristic signals). ¹H NMR δ=3.74 (s, 3H, OCH₃), 4.31–4.47 (m, 2H, C=NCH₂), 5.13 (s, 2H,

COOCH₂), 9.80 (br s, 1H, OH), 10.00 (br s, 1H, HNCOOCH₂). ¹³C NMR δ=54.9 (C=NCH₂), 55.3 (OCH₃), 65.9 (COOCH₂).

4.2.14. Compound **2dB** (minor tautomer, characteristic signals). ¹H NMR δ=4.61–4.68 (m, 1H, CHNHCH), 5.01–5.12 (m, 2H, COOCH₂), 5.61–5.65 (m, 2H, NphCHNH, HNCHO), 9.13 (br s, 1H, HNCOOCH₂). ¹³C NMR δ=52.0 (NphCHNH), 66.0 (COOCH₂), 78.5 (HNCHO).

4.2.15. Compound **2e**. White crystals, yield: 0.92 g (57%), mp: 201–203 °C. HR-EIMS: *m/z* calcd for C₃₆H₂₈N₂O₃: 536.2094, found 536.2091.

4.2.16. Compound **2eA**¹ (major tautomer). ¹H NMR (600 MHz, DMSO) δ=5.15–5.30 (m, 2H, COOCH₂), 6.70 (t, 1H, 7-H, J=7.6 Hz), 6.99 (t, 1H, 6-H, J=7.4 Hz), 7.11 (t, 1H, 5'-H, J=7.5 Hz), 7.25–7.44 (m, 9H, 4''-H, NphCH, 3-H, 7'''-H, 3''-H, 5''-H, 6'''-H, 2''-H, 6''-H), 7.45–7.51 (m, 2H, 4'-H, 3'''-H), 7.60 (d, 1H, 6'-H, J=7.6 Hz), 7.63 (d, 1H, 5-H, J=8.0 Hz), 7.71 (d, 1H, 4-H, J=8.6 Hz), 7.84 (d, 1H, 4'''-H, J=8.2 Hz), 7.88 (d, 1H, 5'''-H, J=8.6 Hz), 8.07 (d, 1H, 2'''-H, J=7.2 Hz), 8.21 (d, 1H, 8'''-H, J=8.6 Hz), 8.25 (d, 1H, 8-H, J=8.7 Hz), 8.28 (d, 1H, 3'-H, J=8.4 Hz), 8.88 (s, 1H, N=CH), 10.58 (br s, 1H, OH), 12.74 (s, 1H, NH). ¹³C NMR (150 MHz, DMSO): δ=66.1 (COOCH₂), 66.2 (NphCH), 117.5 (C-3'), 118.2 (C-3), 119.7 (C-1), 120.6 (C-1'), 122.1 (C-5'), 122.3 (C-6), 123.6 (C-8'''), 124.6 (C-8), 124.9 (C-2'''), 125.2 (C-3'''), 125.5 (C-6'''), 125.6 (C-7), 125.9 (C-7'''), 127.5 (C-4'''), 127.7 (C-4''), 127.9 (C-2'', C-6''), 128.3 (C-5), 128.5 (C-3'', C-5''), 128.7 (C-5'''), 128.8 (C-4a), 129.8 (C-4), 130.6 (C-8a'''), 131.9 (C-4'), 132.4 (C-8a), 133.6 (C-4a'''), 134.0 (C-6'), 136.5 (C-1''), 139.1 (C-1'''), 139.6 (C-2'), 152.1 (COH), 153.3 (COOCH₂), 165.0 (N=CH).

4.2.17. Compound **2eB** (minor tautomer, characteristic signals). ¹H NMR δ=4.54–4.60 (m, 2H, COOCH₂), 4.67–4.73 (m, 1H, CHNHCH), 5.80 (d, 1H, HNCHO, J=13.6 Hz), 6.46 (s, 1H, NphCHNH), 8.11 (br s, 1H, HNCOOCH₂). ¹³C NMR δ=49.7 (NphCHNH), 65.3 (COOCH₂), 78.6 (HNCHO).

4.2.18. Compound **2f**. White crystals, yield: 0.98 (61%), mp: 163–165 °C. HR-EIMS: *m/z* calcd for C₃₆H₂₈N₂O₃: 536.2094, found 536.2097.

4.2.19. Compound **2fA**¹ (major tautomer). ¹H NMR (600 MHz, DMSO) δ=5.17–5.32 (m, 2H, COOCH₂), 6.70 (t, 1H, 7-H, J=7.6 Hz), 6.95 (s, 1H, NphCH), 7.01 (t, 1H, 6-H, J=7.4 Hz), 7.12 (t, 1H, 5'-H, J=7.5 Hz), 7.17 (t, 2H, 3''-H, 5''-H, J=7.5 Hz), 7.24 (t, 1H, 4''-H, J=7.4 Hz), 7.31–7.36 (m, 4H, 3-H, 3'''-H, 2''-H, 6''-H), 7.42–7.49 (m, 3H, 7'''-H, 6'''-H, 4'-H), 7.62 (d, 1H, 6'-H, J=7.6 Hz), 7.69 (d, 1H, 5-H, J=8.1 Hz), 7.73–7.78 (m, 3H, 4'''-H, 4-H, 8'''-H), 7.83 (d, 1H, 5'''-H, J=7.8 Hz), 7.89 (d, 1H, 1'''-H, J=8.2 Hz), 7.96 (d, 1H, 8-H, J=8.7 Hz), 8.31 (d, 1H, 3'-H, J=8.4 Hz), 8.81 (s, 1H, N=CH), 10.25 (br s, 1H, OH), 12.74 (s, 1H, NH). ¹³C NMR (150 MHz, DMSO): δ=66.1 (COOCH₂), 67.3 (NphCH), 117.4 (C-3'), 118.1 (C-3), 119.6 (C-1), 120.5 (C-1'), 122.1 (C-5'), 122.3 (C-6), 123.9 (C-1'''), 124.8 (C-3'''), 125.3 (C-8), 125.6 (C-7), 125.7 (C-6'''), 126.2 (C-7'''), 127.4 (C-5'''), 127.7 (C-2'', C-6''), 127.8 (C-8'''), 127.9 (C-4'', C-4'''), 128.0 (C-8a'''), 128.3 (C-5), 128.4 (C-3'', C-5''), 128.9 (C-4a), 129.7 (C-4), 131.7 (C-8a), 131.8 (C-4a'''), 131.9 (C-4'), 134.1 (C-6'), 136.5 (C-1''), 139.7 (C-2'), 141.1 (C-2'''), 152.9 (COH), 153.4 (COOCH₂), 166.1 (N=CH).

4.2.20. Compound **2fA**² (minor tautomer, characteristic signals). ¹H NMR δ=4.39–4.52 (m, 2H, C=NCH₂), 5.11 (s, 2H, COOCH₂), 9.60 (br s, 1H, OH), 10.07 (br s, 1H, HNCOOCH₂). ¹³C NMR δ=54.8 (C=NCH₂), 65.8 (COOCH₂).

4.2.21. Compound **2fB** (minor tautomer, characteristic signals). ¹H NMR δ=4.71–4.91 (m, 2H, COOCH₂), 4.75–4.80 (m, 1H, CHNHCH), 5.71 (d, 1H, HNCHO, J=13.2 Hz), 5.81 (s, 1H, NphCHNH), 8.92 (br s,

1H, H_NCOOCH₂), ¹³C NMR δ=53.0 (NphCHNH), 65.9 (COOCH₂), 78.5 (HNCHO).

4.3. General method for the synthesis of naphthoxazinoquinazolin-13-ones (3a–f)

Benzoyloxycarbonyl-protected intermediates (**3a–f**) (0.4 mmol) were heated with MeONa (30 or 60 mol %) under solvent-free conditions at their melting temperatures. After a reaction time of 10–40 min, when TLC showed no presence of the starting materials, the reaction mixture was cooled down and the products (**3a–e**) were isolated by treatment with EtOH (15 mL). The white crystals that separated out were filtered off and recrystallized from *i*Pr₂O (10 mL). In the case of compound **3f**, the solid residue was extracted with EtOAc (3 x 10 mL). The combined organic extracts were dried (Na₂SO₄) and concentrated under reduced pressure. The residue was crystallized from *i*Pr₂O and recrystallized from *n*-hexane:EtOAc (10 mL:1 mL). The reaction conditions applied and the yields of **3a–f** are listed in Table 5.

Table 5
Reaction conditions used for the syntheses of **3a–f** and the isolated yields

Products	MeONa (mol %)	Reaction time (min)	Temperature ^a (°C)	Yield ^b (%)
3a	30	10	174	70
3b	30	20	179	61
3c	30	30	152	54
3d	30	65	154	31
3d	60	40	154	60
3e	30	15	203	74
3f	30	30	165	37
3f	60	20	165	51

^a The reactions were performed at the melting temperatures of **2a–f**.

^b Isolated yields.

4.3.1. 7aH,12H,15bH-Naphth[1,2-e][1,3]oxazino[3,2-c]quinazolin-13-one (3a). White crystals, mp: 268–270 °C ¹H NMR (600 MHz, DMSO): δ=4.77 (d, 1H, 15-H_{eq}, J=16.7 Hz), 5.71 (d, 1H, 15-H_{ax}, J=16.7 Hz), 6.63 (s, 1H, 7a-H), 6.98 (d, 1H, 11-H, J=8.1 Hz), 7.04 (d, 1H, 6-H, J=8.8 Hz), 7.09 (t, 1H, 9-H, J=7.5 Hz), 7.41 (t, 1H, 10-H, J=7.8 Hz), 7.44 (t, 1H, 3-H, J=7.5 Hz), 7.51 (d, 1H, 8-H, J=7.6 Hz), 7.58 (t, 1H, 2-H, J=7.6 Hz), 7.77 (d, 1H, 5-H, J=8.9 Hz), 7.84 (d, 1H, 1-H, J=8.4 Hz), 7.88 (d, 1H, 4-H, J=8.1 Hz), 10.22 (br s, 1H, NH). ¹³C NMR (150 MHz, DMSO): δ=40.7 (CH₂), 82.7 (C-7a), 113.0 (C-15a), 114.1 (C-11), 114.8 (C-7b), 118.6 (C-6), 121.6 (C-1), 121.8 (C-9), 124.1 (C-3), 127.1 (C-2), 128.3 (C-4a), 128.4 (C-8), 128.5 (C-5), 128.7 (C-4), 130.6 (C-15b), 130.8 (C-10), 137.0 (C-11a), 151.2 (NCONH), 151.6 (C-6a). HR-EIMS: *m/z* calcd for C₁₉H₁₄N₂O₂: 302.1050, found 302.1058.

4.3.2. (15S*,7aR*)-15-(4-Chlorophenyl)-7aH,12H,15bH-naphth[1,2-e][1,3]oxazino[3,2-c]quinazolin-13-one (3b). White crystals, mp: 292–294 °C ¹H NMR (600 MHz, DMSO): δ=6.29 (s, 1H, 7a-H), 6.98 (d, 1H, 11-H, J=8.2 Hz), 7.05 (t, 1H, 9-H, J=7.5 Hz), 7.15 (d, 1H, 6-H, J=8.9 Hz), 7.19 (s, 1H, PhCH), 7.30 (d, 2H, 2'-H, 6'-H, J=8.0 Hz), 7.37–7.45 (m, 6H, 3-H, 10-H, 1-H, 3'-H, 5'-H, 2-H), 7.51 (d, 1H, 8-H, J=7.7 Hz), 7.92 (d, 2H, 4-H, 5-H, J=8.9 Hz), 10.39 (br s, 1H, NH). ¹³C NMR (150 MHz, DMSO): δ=50.9 (PhCH), 78.5 (C-7a), 112.2 (C-15a), 114.1 (C-11), 114.4 (C-7b), 118.7 (C-6), 121.9 (C-9), 122.7 (C-1), 124.0 (C-3), 127.3 (C-2), 128.6 (C-8), 128.8 (C-4), 128.9 (C-4a, C-3', C-5'), 130.1 (C-5), 130.5 (C-2', C-6'), 130.9 (C-10), 131.0 (C-15b), 132.8 (C-11a), 136.6 (C-11a), 139.6 (C-1'), 150.8 (NCONH), 151.6 (C-6a). HR-EIMS: *m/z* calcd for C₂₅H₁₇ClN₂O₂: 412.0973, found 412.0971.

4.3.3. (15S*,7aR*)-15-Phenyl-7aH,12H,15bH-naphth[1,2-e][1,3]oxazino[3,2-c]quinazolin-13-one (3c). White crystals, mp: 279–281 °C ¹H NMR (600 MHz, DMSO): δ=6.31 (s, 1H, 7a-H), 6.97 (d, 1H, 11-H,

J=8.0 Hz), 7.04 (t, 1H, 9-H, J=7.6 Hz), 7.15 (d, 1H, 6-H, J=9.1 Hz), 7.21 (s, 1H, PhCH), 7.30 (d, 2H, 2'-H, 6'-H, J=7.5 Hz), 7.32–7.42 (m, 7H, 3-H, 3'-H, 4'-H, 5'-H, 10-H, 1-H, 2-H), 7.51 (d, 1H, 8-H, J=7.6 Hz), 7.91 (d, 2H, 4-H, 5-H, J=8.7 Hz), 10.36 (br s, 1H, NH). ¹³C NMR (150 MHz, DMSO): δ=51.5 (PhCH), 78.5 (C-7a), 112.7 (C-15a), 114.1 (C-11), 114.4 (C-7b), 118.7 (C-6), 121.9 (C-9), 122.8 (C-1), 124.0 (C-3), 127.2 (C-2), 128.1 (C-4'), 128.6 (C-8), 128.7 (C-5, C-2', C-6'), 128.8 (C-3', C-5'), 128.9 (C-4a), 129.9 (C-4), 130.9 (C-10), 131.0 (C-15b), 136.6 (C-11a), 140.8 (C-1'), 150.8 (NCONH), 151.5 (C-6a). HR-EIMS: *m/z* calcd for C₂₅H₁₈N₂O₂: 378.1363, found 378.1343.

4.3.4. (15S*,7aR*)-15-(4-Methoxyphenyl)-7aH,12H,15bH-naphth[1,2-e][1,3]oxazino[3,2-c]quinazolin-13-one (3d). White crystals, mp: 275–277 °C ¹H NMR (600 MHz, DMSO): δ=3.72 (s, 3H, OCH₃), 6.31 (s, 1H, 7a-H), 6.92 (d, 2H, 3'-H, 5'-H, J=8.3 Hz), 6.97 (d, 1H, 11-H, J=8.1 Hz), 7.04 (t, 1H, 9-H, J=7.5 Hz), 7.12–7.18 (m, 2H, 6-H, PhCH), 7.21 (d, 2H, 2'-H, 6'-H, J=7.9 Hz), 7.35–7.44 (m, 4H, 3-H, 10-H, 2-H, 1-H), 7.51 (d, 1H, 8-H, J=7.6 Hz), 7.87–7.92 (m, 2H, 5-H, 4-H), 10.33 (br s, 1H, NH). ¹³C NMR (150 MHz, DMSO): δ=51.1 (PhCH), 55.1 (OCH₃), 78.4 (C-7a), 113.0 (C-15a), 114.1 (C-11), 114.2 (C-3', C-5'), 114.4 (C-7b), 118.7 (C-6), 121.9 (C-9), 122.9 (C-1), 123.9 (C-3), 127.1 (C-2), 128.6 (C-8), 128.7 (C-4), 128.9 (C-4a), 129.8 (C-5), 129.9 (C-2', C-6'), 130.9 (C-10), 131.0 (C-15b), 132.8 (C-1'), 136.6 (C-11a), 150.8 (NCONH), 151.4 (C-6a), 158.9 (COCH₃). HR-EIMS: *m/z* calcd for C₂₆H₂₀N₂O₃: 408.1468, found 408.1467.

4.3.5. (15S*,7aR*)-15-(Naphthalen-1-yl)-7aH,12H,15bH-naphth[1,2-e][1,3]oxazino[3,2-c]quinazolin-13-one (3e). White crystals, mp: 275–277 °C ¹H NMR (600 MHz, DMSO): δ=6.41 (s, 1H, 7a-H), 6.95–7.02 (m, 2H, 11-H, 9-H), 7.15 (d, 1H, 2'-H, J=7.1 Hz), 7.19 (d, 1H, 6-H, J=8.9 Hz), 7.22 (d, 1H, 1-H, J=8.4 Hz), 7.31 (t, 1H, 2-H, J=7.6 Hz), 7.33–7.42 (m, 3H, 3-H, 10-H, 3'-H), 7.47 (d, 1H, 8-H, J=7.6 Hz), 7.62 (t, 1H, 6'-H, J=7.5 Hz), 7.69 (t, 1H, 7'-H, J=7.6 Hz), 7.88 (s, 1H, NphCH), 7.90–7.97 (m, 3H, 5-H, 4-H, 4'-H), 8.03 (d, 1H, 5'-H, J=8.1 Hz), 8.67 (d, 1H, 8'-H, J=8.6 Hz), 10.49 (br s, 1H, NH). ¹³C NMR (150 MHz, DMSO): δ=49.4 (NphCH), 78.4 (C-7a), 112.9 (C-15a), 114.1 (C-11), 114.8 (C-7b), 118.6 (C-6), 122.0 (C-9), 122.3 (C-1), 123.4 (C-8'), 124.0 (C-3), 125.2 (C-3'), 126.3 (C-6'), 127.0 (C-7'), 127.3 (C-2), 128.4 (C-8), 128.8 (C-4), 128.9 (C-5), 129.0 (C-5'), 129.1 (C-4a), 129.2 (C-2'), 130.0 (C-4'), 130.7 (C-8a'), 130.9 (C-10, C-15b), 133.9 (C-4a'), 135.5 (C-1'), 136.6 (C-11a), 151.2 (NCONH), 151.8 (C-6a). HR-EIMS: *m/z* calcd for C₂₉H₂₀N₂O₂: 428.1519, found 428.1522.

4.3.6. (15S*,7aR*)-15-(Naphthalen-2-yl)-7aH,12H,15bH-naphth[1,2-e][1,3]oxazino[3,2-c]quinazolin-13-one (3f). Beige crystals, mp: 273–275 °C ¹H NMR (600 MHz, DMSO): δ=6.40 (s, 1H, 7a-H), 6.96–7.04 (m, 2H, 11-H, 9-H), 7.20 (d, 1H, 6-H, J=9.0 Hz), 7.34–7.40 (m, 4H, 2-H, NphCH, 3-H, 10-H), 7.42–7.54 (m, 4H, 1-H, 7'-H, 8-H, 6'-H), 7.58–7.65 (m, 2H, 3'-H, 1'-H), 7.77 (d, 1H, 8'-H, J=8.1 Hz), 7.88–8.00 (m, 4H, 5'-H, 5-H, 4-H, 4'-H), 10.40 (br s, 1H, NH). ¹³C NMR (150 MHz, DMSO): δ=51.8 (NphCH), 78.5 (C-7a), 112.6 (C-15a), 114.1 (C-11), 114.4 (C-7b), 118.8 (C-6), 121.9 (C-9), 122.8 (C-1), 124.0 (C-3), 126.4 (C-3'), 126.5 (C-7'), 126.6 (C-6'), 127.2 (C-2), 127.6 (C-5'), 127.9 (C-1'), 128.1 (C-8'), 128.6 (C-8), 128.8 (C-5), 128.9 (C-4a, C-4'), 130.1 (C-4), 130.9 (C-10), 131.1 (C-15b), 132.5 (C-4a'), 132.6 (C-8a'), 136.6 (C-11a), 138.2 (C-2'), 150.9 (NCONH), 151.6 (C-6a). HR-EIMS: *m/z* calcd for C₂₉H₂₀N₂O₂: 428.1519, found 428.1543.

Acknowledgements

The authors thank the Hungarian Research Foundation (OTKA No. K-75433) and TÁMOP-4.2.1/B-09/KONV-2010-0005 and the Deutsche Akademische Austauschdienst (DAAD), project-ID 50368559, for financial support. I.S. acknowledges the award of a Bolyai János Fellowship.

References and notes

- (a) Bur, S. K.; Martin, S. F. *Tetrahedron* **2001**, *57*, 3221; (b) Speckamp, W. N.; Moolenaar, M. J. *Tetrahedron* **2000**, *56*, 3817; (c) Arend, M.; Westermann, B.; Risch, N. *Angew. Chem., Int. Ed.* **1998**, *37*, 1045.
- (a) Liras, S.; Davoren, J. E.; Bordner, J. *Org. Lett.* **2001**, *3*, 703; (b) Ito, M.; Clark, C. W.; Mortimore, M.; Goh, J. B.; Martin, S. F. *J. Am. Chem. Soc.* **2001**, *123*, 8003.
- Szatzmári, I.; Fülöp, F. *Curr. Org. Synth.* **2004**, *1*, 155.
- Szatzmári, I.; Hetényi, A.; Lázár, L.; Fülöp, F. *J. Heterocycl. Chem.* **2004**, *41*, 367.
- Heydenreich, M.; Koch, A.; Klod, S.; Szatzmári, I.; Fülöp, F.; Kleinpeter, E. *Tetrahedron* **2006**, *62*, 11081.
- Heydenreich, M.; Koch, A.; Szatzmári, I.; Fülöp, F.; Kleinpeter, E. *Tetrahedron* **2008**, *64*, 7378.
- Szatzmári, I.; Fülöp, F. *Tetrahedron Lett.* **2011**, *52*, 4440.
- Csütörtöki, R.; Szatzmári, I.; Koch, A.; Heydenreich, M.; Kleinpeter, E.; Fülöp, F. *Tetrahedron* **2011**, *67*, 8564.
- (a) Devi, P. U.; Lakshmi, K. A.; Ramji, M. T.; Khan, P. A. *J. Pharm. Res.* **2010**, *3*, 2765; (b) Ram, V. J.; Farhanullah; Tripathi, B. K.; Srivastava, A. K. *Bioorg. Med. Chem.* **2003**, *11*, 2439.
- Sanz, P.; Mó, O.; Yáñez, M.; Elguero, J. *J. Phys. Chem. A* **2007**, *111*, 3585.
- Szatzmári, I.; Martinek, T. A.; Lázár, L.; Fülöp, F. *Tetrahedron* **2003**, *59*, 2877.
- Frisch, M. J.; Trucks, G. W.; Schlegel, H. B.; Scuseria, G. E.; Robb, M. A.; Cheeseman, J. R.; Scalmani, G.; Barone, V.; Mennucci, B.; Petersson, G. A.; Nakatsuji, H.; Caricato, M.; Li, X.; Hratchian, H. P.; Izmaylov, A. F.; Bloino, J.; Zheng, G.; Sonnenberg, J. L.; Hada, M.; Ehara, M.; Toyota, K.; Fukuda, R.; Hasegawa, J.; Ishida, M.; Nakajima, T.; Honda, Y.; Kitao, O.; Nakai, H.; Vreven, T.; Montgomery, T. A.; Peralta, J. E., Jr.; Ogliaro, F.; Bearpark, M.; Heyd, J. J.; Brothers, E.; Kudin, K. N.; Staroverov, V. N.; Kobayashi, R.; Normand, J.; Raghavachari, K.; Rendell, A.; Burant, J. C.; Iyengar, S. S.; Tomasi, J.; Cossi, M.; Rega, N.; Millam, J. M.; Klene, M.; Knox, J. E.; Cross, J. B.; Bakken, V.; Adamo, C.; Jaramillo, J.; Gomperts, R.; Stratmann, R. E.; Yazyev, O.; Austin, A. J.; Cammi, R.; Pomelli, C.; Ochterski, J. W.; Martin, R. L.; Morokuma, K.; Zakrzewski, V. G.; Voth, G. A.; Salvador, P.; Dannenberg, J. J.; Dapprich, S.; Daniels, A. D.; Farkas, O.; Foresman, J. B.; Ortiz, J. V.; Cioslowski, J.; Fox, D. J. *Gaussian 09, Revision A.02*; Gaussian: Wallingford CT, 2009.
- Hehre, W. J.; Radom, L.; von Ragué Schleyer, P.; Pople, J. *Ab Initio Molecular Orbital Theory*; Wiley: New York, NY, 1986.
- Becke, A. D. *J. Chem. Phys.* **1993**, *98*, 1372.
- SYBYL 7.3; Tripos: 1699 South Hanley Road, St. Louis, MO 63144, USA, 2007.
- Klod, S.; Kleinpeter, E. *J. Chem. Soc., Perkin Trans. 2* **2002**, 1893.
- Tóth, G.; Kovács, J.; Lévai, A.; Koch, A.; Kleinpeter, E. *Magn. Reson. Chem.* **2001**, *39*, 251.
- Kovács, J.; Tóth, G.; Simon, A.; Lévai, A.; Koch, A.; Kleinpeter, E. *Magn. Reson. Chem.* **2003**, *41*, 193.
- Kleinpeter, E.; Holzberger, A. *Tetrahedron* **2001**, *57*, 6941.
- Germer, A.; Klod, S.; Peter, M. G.; Kleinpeter, E. *J. Mol. Model.* **2002**, *8*, 231.
- Klod, S.; Koch, A.; Kleinpeter, E. *J. Chem. Soc., Perkin Trans. 2* **2002**, 1506.
- Kleinpeter, E.; Klod, S.; Rudorf, W.-D. *J. Org. Chem.* **2004**, *69*, 4317.
- Kleinpeter, E.; Klod, S. *J. Am. Chem. Soc.* **2004**, *126*, 2231.
- Szatzmári, I.; Martinek, T. A.; Lázár, L.; Koch, A.; Kleinpeter, E.; Neuvonen, K.; Fülöp, F. *J. Org. Chem.* **2004**, *69*, 3645.
- Ryppa, C.; Senge, M. O.; Hatscher, S. S.; Kleinpeter, E.; Wacker, P.; Schilde, U.; Wiehe, A. *Chem.—Eur. J.* **2005**, *11*, 3427.
- (a) Kleinpeter, E.; Schulenburg, A.; Zug, I.; Hartmann, H. *J. Org. Chem.* **2005**, *70*, 6592; (b) Kleinpeter, E.; Schulenburg, A. *J. Org. Chem.* **2006**, *71*, 3869.
- Kleinpeter, E.; Koch, A.; Sahoo, H. S.; Chand, D. K. *Tetrahedron* **2008**, *64*, 5044.
- (a) Kleinpeter, E.; Koch, A.; Seidl, P. R. *J. Phys. Chem. A* **2008**, *112*, 4989; (b) Kleinpeter, E.; Szatzmári, I.; Lázár, L.; Koch, A.; Heydenreich, M.; Fülöp, F. *Tetrahedron* **2009**, *65*, 8021.
- Kleinpeter, E.; Klod, S.; Koch, A. *J. Mol. Struct.: THEOCHEM* **2007**, *811*, 45 and references therein.
- Kleinpeter, E.; Klod, S.; Koch, A. *J. Mol. Struct.: THEOCHEM* **2008**, 857, 89.
- Kleinpeter, E.; Koch, A.; Shainyan, B. A. *J. Mol. Struct.: THEOCHEM* **2008**, 863, 127.
- Kleinpeter, E.; Koch, A. *J. Mol. Struct.: THEOCHEM* **2008**, 851, 313.
- (a) Kleinpeter, E.; Klod, S.; Koch, A. *J. Org. Chem.* **2008**, *73*, 1498; (b) Kleinpeter, E.; Koch, A. *J. Mol. Struct.: THEOCHEM* **2010**, 939, 1.
- Kleinpeter, E.; Koch, A. *Phys. Chem. Chem. Phys.* **2011**, *13*, 20593.
- (a) Stewart, J. J. P. *J. Comput. Chem.* **1989**, *10*, 209; (b) Stewart, J. J. P. *J. Comput. Chem.* **1989**, *10*, 221.
- Becke, A. D. *J. Chem. Phys.* **1993**, *98*, 5648.
- Lee, C.; Yang, W.; Parr, R. G. *Phys. Rev. B* **1988**, *37*, 785.
- Tomasi, J.; Mennucci, B.; Cammi, R. *Chem. Rev.* **2005**, *105*, 2999.
- Gauss View 2.0; Gaussian; 2000 Carnegie Office Park, Building 6, Pittsburgh, PA 15106, USA.
- Tóth, D.; Szatzmári, I.; Heydenreich, M.; Koch, A.; Kleinpeter, E.; Fülöp, F. *J. Mol. Struct.* **2009**, 929, 58.
- Diedrich, C. L. *Eur. J. Org. Chem.* **2008**, *10*, 1811.
- Waibel, M.; Hasserodt, J. *Tetrahedron Lett.* **2009**, *50*, 2767.
- Walji, D. V. B.; Storey, J. M. D.; Harrison, W. T. A. *Acta Crystallogr.* **2007**, *63*, 2120.